ordering[17,19,20] of $xy > z^2 > xz > yz > x^2 - y^2$ the ground state ^2A_g has the hole configuration $(xy)^2(z^2)^1$. Under D_{2h} symmetry, $z^2(a_g)$ and $x^2 - y^2(a_g)$ will mix and the admixture seems to be small as revealed by very small orthorombicity in the ESR spin-Hamiltonian parameters.[19] All the excitations must be spin allowed. Spin-allowed transitions can be obtained by promoting electrons from z^2 to xy and from the filled d levels to the half-filled z^2 orbital or to the empty xy orbital. The one-electron transitions, vacancy configurations, the spectroscopic ground and excited states, and the interelectronic repulsion energies associated with them are listed in Table II. From Table II it is clear that the first band at 15 260 cm^{-1} can be unequivocally assigned to $^2A_g \rightarrow {}^2B_{1g}$ ($z^2 \rightarrow xy$) with an enabling vibration B_{2u} and/or B_{3u}. This assignment accounts for perpendicular polarization. However, a small admixture with an enabling vibration A_u cannot be ruled out, which would give this transition parallel polarization. Similarly, the band at 21 640 cm^{-1} can be a combination band from $^2A_g \rightarrow {}^2B_{3g}{}^{(2)}$ and $^2A_g \rightarrow {}^2B_{2g}{}^{(1)}$ resulting from the excitations $xz \rightarrow xy$ and $yz \rightarrow xy$, and the large intensity band at 23 650 cm^{-1} can be a combination of up to three different bands $^2A_g \rightarrow {}^2A_g$ ($x^2 - y^2 \rightarrow z^2$), $^2A_g \rightarrow {}^2B_{2g}{}^{(2)}$ ($yz \rightarrow xy$), and $^2A_g \rightarrow {}^2B_{1g}{}^{(2)}$ ($x^2 - y^2 \rightarrow xy$), since these bands are all mainly parallel polarized. Finally the band at 24,800 cm^{-1} can be assigned to $^2A_g \rightarrow {}^2B_{1g}{}^{(2)}$ ($x^2 - y^2 \rightarrow xy$). The entire assignment and justification for polarizations are given in Table II. The band observed at 28 420 cm^{-1} should be of ligand $\rightarrow$ metal origin.

A calculation using the Wolfsberg–Helmholz molecular orbital method was performed with the valence orbitals of ligands and metal as the basis functions. The energy level ordering obtained is $xy > z^2 > yz + L \sim xy + L > x^2 - y^2 > yz \sim xz$. The d orbitals appearing above and below $x^2 - y^2$ with varying amounts of admixture simply suggest the delocalized nature of the electrons in these orbitals. We presume that the WHMO calculation has underestimated the d–orbital populations in the molecular orbitals appearing above $x^2 - y^2$. It is, however, interesting to note that the ordering of the levels and the ground state predicted by WHMO calculation is consistent with our spectral assignments.

Acknowledgment. We gratefully acknowledge the Department of Science and Technology, Government of India, for the financial support to carry out this work.

Registry No. $[Ni(dp)_2Cl_2]PF_6$, 94701-86-7.

Contribution from the Central Research Institute for Chemistry, Budapest, H-1525 Hungary, and Institute of Organic Chemistry, Veszprém University of Chemical Engineering, H-8201 Veszprém, Hungary

Electron Spin Resonance Investigation of Copper(I)–9,10-Phenanthrenesemiquinonate Complexes

A. Rockenbauer,*† M. Györ,† G. Speier,‡ and Z. Tyeklár‡

Received March 5, 1987

Electron spin resonance spectra of copper(I) complexes with the structures of $[CuL_2(SQ)]$ and $[CuL(SQ)]$ have been investigated in different solvents, where SQ is substituted 9,10-phenanthrenesemiquinonate and L is triphenylphosphine. The well-resolved hyperfine patterns of ^{63}Cu, ^{65}Cu, ^{31}P, and protons of SQ were analyzed by computer simulations. The spectral parameters of mono complexes in coordinating solvents were found intermediate between the data of mono- and bis(phosphine) complexes in noncoordinating solvents. The spin densities on the Cu and P atoms and SQ ring were found to vary oppositely, which could be expected from the electron affinity and half-wave potential of SQ. This anomaly was explained by a three-electron bonding scheme between one filled 3d orbital of copper and the delocalized π-system of SQ, which suggests opposite direction of the spin and charge transport between the metal ion and SQ.

Introduction

The electron spin resonance (ESR) spectra of various (*o*-semiquinonato)copper(I) complexes with neutral ligands have been investigated by Razuvaev et al.[1] They classified these complexes as radicals since the unpaired electron is mainly localized on the *o*-semiquinonate ligands (SQ). There is, however, a small fraction of spin density on the central ion and the neutral ligands (L) too, which yields hyperfine splitting due to the couplings of ^{63}Cu, ^{65}Cu, and ^{31}P nuclei. These couplings were found to depend sensitively on the coordination number of copper ion: for complexes [CuL(SQ)] with trigonal geometry small splittings were observed, while for the complexes $[CuL_2(SQ)]$ with tetrahedral geometry large splittings were observed. In the latter case the couplings of ^{63}Cu, ^{65}Cu, and ^{31}P nuclei vary anomalously with the electron affinity of SQ: the larger the electron affinity, the larger the spin density that can be observed on the metal ion and neutral ligand.

In order to obtain further details of the spin distribution in complexes with the structure $[CuL_n(SQ)]$ ($n = 1$ or 2), we studied substituted copper(I)–9,10–phenanthrenesemiquinonate complexes with the neutral ligand triphenylphosphine.

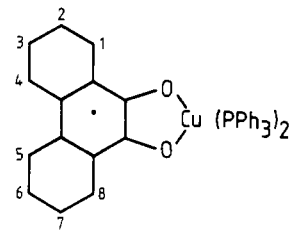

Since the *o*-semiquinone ligand possesses a large delocalized π-electron system, not only can we study the variation of spin densities on the metal ion and neutral ligands but information can also be obtained from the rearrangement of spin distribution on SQ, when different substituents are applied.

Experimental Section

All reactions were carried out under an atmosphere of pure, dry argon with the use of standard Schlenk-type glassware and techniques. 9,10-Phenanthrenequinone (Fluka), triphenylphosphine (Fluka), and copper powder (Reanal) were used as supplied. 1-Nitro-9,10-phenanthrenequinone,[2] 2-nitro-9,10-phenanthrenequinone,[3] 3-nitro-9,10-

† Central Research Institute for Chemistry.
‡ Veszprém University of Chemical Engineering.

(1) Razuvaev, G. V.; Cherkasov, V. K.; Abakumov, G. A. *J. Organomet. Chem.* **1978**, *160*, 361.
(2) Dewar, M. J. S.; Warford, E. W. T. *J. Chem. Soc.* **1956**, 3570.

0020-1669/87/1326-3293$01.50/0

Table I. Characterization of $[Cu(SQ)(PPh_3)_2]$ Complexes

no.	complex	yield, %	mp, °C	elemental anal.,[a] % C	H	N	P	Cu	μ_{eff}	vis spectrum,[c] cm^{-1} (dm^3 mol^{-1} cm^{-1})
1	SQ	87	159–162	75.3 (75.4)	4.8 (4.8)		7.7 (7.8)	8.7 (8.6)	1.75	30200 (8356), 26250 sh (4266), 24900 (4443), 20200 (3270), 18850 sh (3027), 14200 (1276)
2	1-NO_2-SQ	76	147	69.8 (71.4)	4.2 (4.4)	1.9 (1.7)	7.3 (7.4)	7.9 (7.6)	1.78	30100 (6711), 26350 (3442), 24620 sh (3132), 18800 (2906), 15200 (2802)
3	2-NO_2-SQ	69	144–145	71.3 (71.4)	4.4 (4.4)	1.8 (1.7)	7.6 (7.4)	7.5 (7.6)	1.71	24480 sh (4984), 20100 (4684), 19100 sh (4439), 13270 (2991)
4	3-NO_2-SQ	63	154–156	69.6 (71.4)	4.2 (4.4)	1.8 (1.7)	7.5 (7.4)	7.7 (7.6)	1.72	29700 sh (7929), 26350 (4677), 24600 (4535), 19200 (3982), 13700 (4000)
5	4-NO_2-SQ	83	126–127	71.1 (71.4)	41.5 (4.4)	1.6 (1.7)	7.2 (7.4)	7.4 (7.6)	1.73	25000 (5320), 19750 (5477), 19000 (5441) 14400 (2696)
6	2,7-$(NO_2)_2$-SQ	80	168–169	67.7 (67.7)	4.1 (4.1)	3.7 (3.2)	6.9 (7.0)	7.3 (7.2)	1.75	19460 sh (6777), 18490 (7337), 12670 (2904)
7	2,7-(*t*-Bu)$_2$-SQ	89	112–114	72.5 (72.3)	6.0 (6.0)		6.7 (6.8)	6.9 (7.0)	1.85	30100 sh (5380), 24300 (2813), 18700 sh (9680), 14400 (7530)

[a] Calculated data in parentheses. [b] At 298.2 K. [c] In benzene.

phenanthrenequinone,[4] 4-nitro-9,10-phenanthrenequinone,[5] 2,7-dinitro-9,10-phenanthrenequinone,[6] and 2,7-di-*tert*-butyl-9,10-phenanthrenequinone[7] were prepared by known methods. The unsubstituted 9,10-phenanthrenesemiquinonate complexes $[Cu(SQ)(PPh_3)_2]$[8] and $[Cu(SQ)(PPh_3)]_2$[9] were prepared according to literature methods. The substituted 9,10-phenanthrenesemiquinonate complexes of the formula $[Cu(SQ)(PPh_3)_2]$ were prepared in an analogous manner. Their characterization is summarized in Table I. Solvents were dried by standard methods and distilled before use.

The vis spectra were recorded on a Specord M 40 (Carl Zeiss, Jena, East Germany) spectrometer. The magnetic susceptibilities were determined on a Bruker B-E 10B8 magnetic susceptibility system. The half-wave potentials of the quinones were determined by cyclic voltammetry in a 0.1 M tetrabutylammonium perchlorate–dichloromethane solution, using ferrocene as the internal standard on a CV-1B cyclic voltammograph (Bioanalytical Systems Inc.).

The ESR spectra were recorded on a JEOL type JES-FE/3X spectrometer in X microwave band with 100-kHz field modulation at room temperture. In order to obtain good resolution, benzene solutions after careful degassing were investigated and low concentrations were chosen to avoid line broadening due to spin–spin interactions.

Results

The spectra were evaluated by computer simulations. A FORTRAN program was written for a KFKI (Budapest, Hungary) produced EMU 11 minicomputer to simulate isotropic ESR spectra with an arbitrary number of hyperfine splittings. In the spectra of the complexes $[CuL_2(SQ)]$ the primary structure consists of six complex patterns due to the nearly identical splittings of one Cu nucleus ($I = {}^3/_2$) and two ^{31}P nuclei ($I = {}^1/_2$). Each pattern has a complex secondary structure due to the couplings of semiquinone protons (maximum eight) and the difference between the ^{63}Cu and ^{65}Cu couplings. The computed spectra were built up as a superposition of the ^{63}Cu and ^{65}Cu spectra with weighting factors 0.692 and 0.308, respectively. In order to obtain reliable values for the small proton couplings, the two outermost line patterns were simulated separately on an expanded field scale.

The unique determination of proton couplings requires only a fine tuning of parameters in the simulation procedure if the spectra of nonsubstituted or 2,7-disubstituted complexes are analyzed, where the large a_1, a_3, a_6, a_8 and small a_2, a_4, a_5, a_7 couplings are equivalent in pairs and the respective patterns are well separated. In the case of monosubstitution, where no protons are equivalent, all of the large and small couplings were systematically varied in steps of 0.005 mT and the best three simulations were selected. Then the parameters were changed in steps of 0.002 mT in order to achieve good agreement between the calculated and experimental spectra. An example of the simulation is shown in Figure 1.

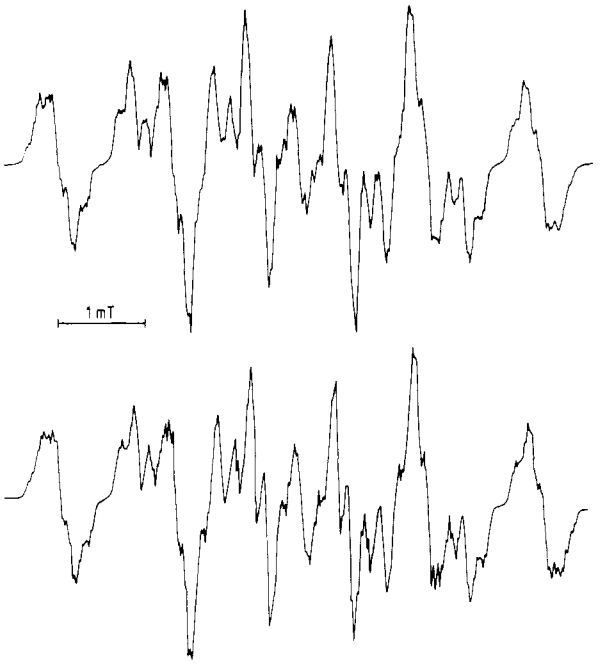

Figure 1. ESR spectra of $[Cu(3\text{-}NO_2SQ)L_2]$: top, experimental; bottom, calculated with parameters in Table III.

Table II. Magnetic Parameters of [CuL(SQ)] Complexes in Various Solvents

solvent	g[b]	hyperfine couplings, mT[a] Cu[c]	P[c]	H(4)[d]	H(4)[d]
pyridine	2.0050	0.666	0.700		
DMSO	2.0035	0.440	0.250	0.16	0.03
CH_2Cl_2	2.0037	0.305	0.165	0.16	0.03

[a] The hyperfine constants can be converted into cm^{-1} units by the formula a (cm^{-1}) = (a (mT))g/2142. [b] The error is 0.0001. [c] The error is 0.002 mT. [d] The error is 0.01 mT.

Solvent Effects. In order to study the effect of coordination on the spin distribution, we dissolved the $[CuL_2(SQ)]$ complex in different solvents. In noncoordinating solvent (benzene), an ESR signal with the six-line pattern characteristic of the $[Cu(SQ)L_2]$ complex can be observed, while in strongly coordinating solvent (pyridine), the spectrum consists of the five-line pattern of the [Cu(SQ)L] complex. In solvents of intermediate coordi-

(3) Schmidt, J.; Austin, P. C. *Chem. Ber.* **1903**, *36*, 3731.
(4) Braithwaite, R. S. W.; Holt, P. F. *J. Chem. Soc.* **1959**, 2304.
(5) Schmidt, J.; Schraiver, O. *Chem. Ber.* **1911**, *44*, 740.
(6) Schmidt, J.; Kämpf, J. *Chem. Ber.* **1903**, *36*, 3738.
(7) Buu-Hoi, Ng. Ph.; Cagniant, P. *Chem. Ber.* **1944**, *77*, 121.
(8) Kucsera, S.; Speier, G.; Tyeklár, Z.; Hendrickson, D. N., submitted for publication in *Inorg. Chem.*
(9) Kucsera, S.; Speier, G.; Tyeklár, Z.; Hendrickson, D. N., submitted for publication in *J. Am. Chem. Soc.*

Table III. Magnetic Parameters for Substituted $[CuL_2(SQ)]$ Complexes in Benzene

parameter[a]	unit	anion radical[a]	substituents						
			none	2,7-$(NO_2)_2$	2,7-(*t*-Bu)$_2$	2-NO_2	4-NO_2	1-NO_2	3-NO_2
a_1	mT[b]	0.135	0.152	0.178	0.151	0.200	0.150		0.174
a_2	mT	0.020	0.035				0.022	0.064	0.050
a_3	mT	0.167	0.152	0.113	0.158	0.148	0.137	0.174	
a_4	mT	0.042	0.035	0.041	0.040	0.050		0.050	0.064
a_5	mT	0.042	0.035	0.041	0.040	0.023	0.028	0.033	0.033
a_6	mT	0.167	0.152	0.113	0.158	0.130	0.137	0.127	0.127
a_7	mT	0.020	0.035			0.023	0.028	0.023	0.033
a_8	mT	0.135	0.152	0.178	0.151	0.130	0.137	0.127	0.127
$a(^{63}Cu)$	mT		0.895	0.950	0.867	0.920	0.922	0.920	0.920
$a(^{65}Cu)$	mT		0.959	1.018	0.929	0.985	0.987	0.985	0.985
$a(^{31}P)$	mT		1.240	1.370	1.170	1.284	1.307	1.324	1.324
g		2.0046[c]	2.0046	2.0052	2.0045	2.0049	2.0049	2.0052	2.0051

[a] The error of hyperfine constants is 0.002 mT; the error of g values is 0.0001. Data are taken from ref 12. [b] Can be converted by the formula a (cm^{-1}) = (a (mT))g/2142. [c] In H_2O from ref 13.

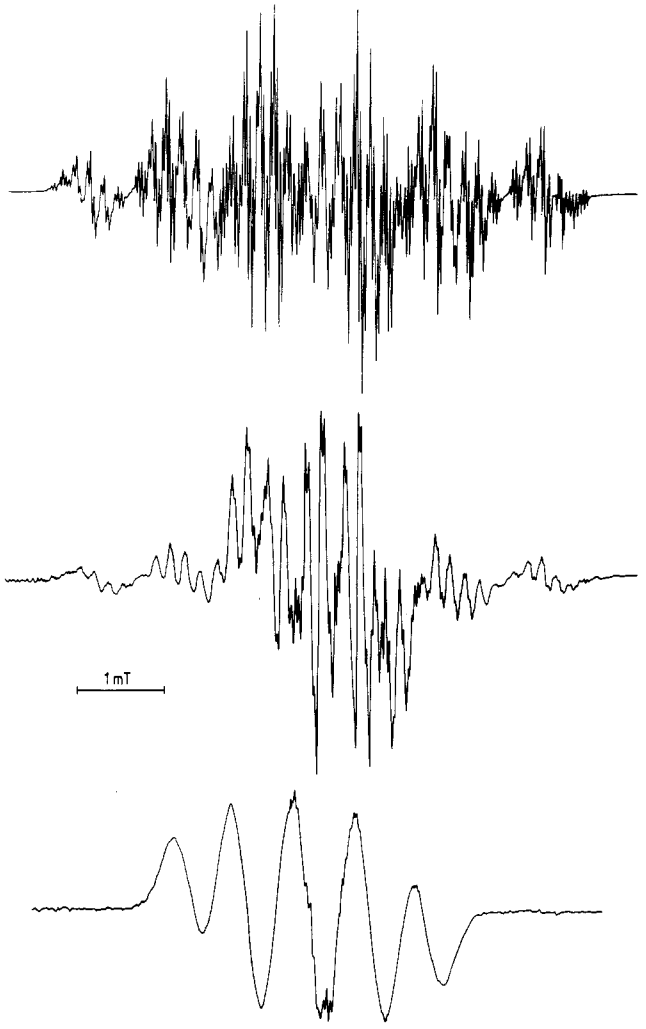

Figure 2. ESR spectra of $[CuL_n(SQ)]$ complexes: top, in benzene; middle, in DMSO; bottom, in pyridine solutions.

nating strength (CH_2Cl_2 and dimethyl sulfoxide), a superposition of signals of both complexes appeared (Figure 2). The spectral parameters of these complexes are given in Table II. In Figure 3 the ^{63}Cu coupling is plotted vs. the ^{31}P coupling. The figure also shows the linear relationship between these coupling constants and those obtained by Razuvaev[1] for other (*o*-semiquinonato)-copper(I) complexes with triphenylphosphine ligands:

$$A(Cu) = 0.34\ mT + 0.44A(P) \quad (1)$$

Our data fit remarkably well to the Razuvaev equation, which was originally based on the spectral data of other $[Cu(SQ)L_2]$ complexes. The large extent of solvent dependence indicates a solvent coordination of the mono(triphenylphosphine) complexes

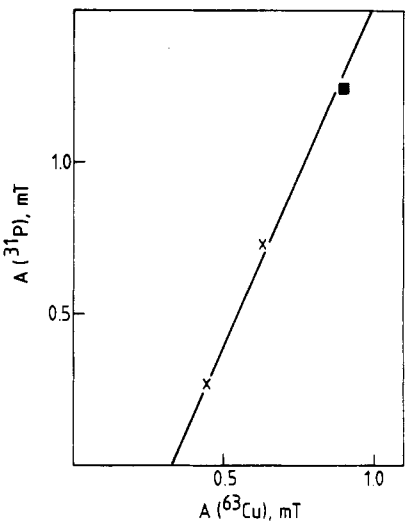

Figure 3. Plot of $A(^{31}P)$ vs. $A(^{63}Cu)$ for the complexes $[CuL_n(SQ)]$: ×, for n = 1 in DMSO and pyridine; ■, for n = 2 in benzene. The straight line represents the Razuvaev's equation.

to give [CuL(S)(SQ)], where S stands for the solvent molecule. The spectral parameters of this solvent-coordinated complex vary between the ones of [CuL(SQ)] and $[CuL_2(SQ)]$ and can approach the data of the bis(triphenylphosphine) complex if the solvent coordination is strong.

Substituent Effects. Substituents with electron-attracting properties, like NO_2, will increase and those with electron-donating properties, like the *tert*-butyl (*t*-Bu) group, will decrease the electron affinity of phenanthrenequinone. The half-wave potential ($E_{1/2}$) changing linearly with the affinity[10] can be used for the characterization of the substituent effect when the substitution is carried out at different positions of SQ. The effect of substituents for magnetic parameters derived from the ESR spectra of $[CuL_2(SQ)]$ complexes in benzene is shown in Table III. For the sake of comparison, Table III also includes the respective parameters of the phenanthrenequinone anion radical.[11,12]

The general feature of substituent effects is the linear dependence of magnetic parameters on the half-wave potential, which is demonstrated in Figure 4. If the electron affinity is strong, i.e., $E_{1/2}$ is less negative, large copper and phosphorus couplings, as well as g values, can be observed. On the other hand, the sum of the four large proton couplings of SQ, namely $a_1 + a_3 + a_6 + a_8$, decreases if the affinity of SQ is increased by 2-NO_2 and 2,7-$(NO_2)_2$ substitutions (see Table III). In case of electron-donating substitution (2,7-(*t*-Bu)$_2$), just the opposite trends can be seen. Consequently, the increasing electron affinity of SQ

(10) Mukherjee, T. K. *J. Phys. Chem.* **1967**, *71*, 2277.
(11) Vincow, G.; Fraenkel, G. K. *J. Chem. Phys.* **1961**, *34*, 1333.
(12) Dehl, R.; Fraenkel, G. K. *J. Chem. Phys.* **1963**, *39*, 1793.

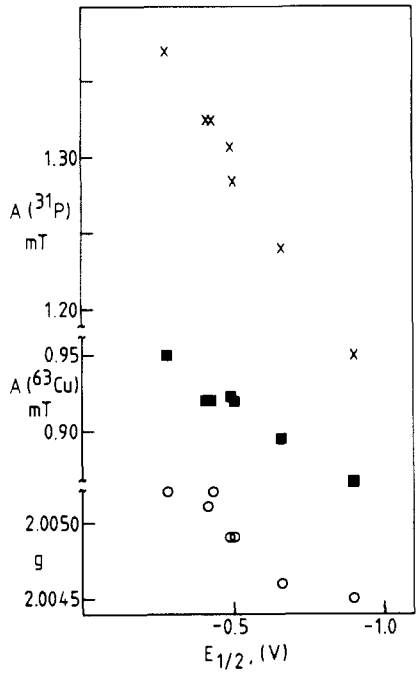

Figure 4. Variation of g, $A(^{31}P)$, and $A(^{63}Cu)$ as a function of $E_{1/2}$ half-wave potential of semiquinone for the complexes $[CuL_2(SQ)]$.

transfers spin density from the semiquinone moiety into the metal ion and neutral ligand.

This transfer of spin density, however, affects the spin distribution on SQ nonuniformly. This is evidenced in Table III through the variation of individual proton couplings and the direction of g variations. Prabhananda[13] suggested a method of deriving spin density from the g value of semiquinone anion radicals. It has been found that the major contribution to the g value comes from the spin density of the oxygen atoms. Since the g values of $[CuL_2(SQ)]$ complexes and the semiquinone radical ions are nearly identical, it is reasonable to attribute the variation of g values of the complexes to the change of spin density of the oxygen atoms. This means the increase of g with the electron affinity in Figure 4 can be explained by the enhancement of oxygen spin density. Consequently, the spin density on the oxygen atoms varies in the direction opposite to that of the carbon skeleton of SQ.

The rearrangement of spin distribution on SQ can be demonstrated by comparing the couplings $a_{3,6}$ and $a_{1,8}$ in the anion radical and the complex. In the case of the anion radical, larger proton couplings were measured at the positions farther from the oxygen atoms

$$a_{3,6} > a_{1,8} \tag{2}$$

while in the case of the nonsubstituted complex

$$a_{3,6} = a_{1,8} \tag{3}$$

i.e., four identical couplings were obtained. This means the complex formation is accompanied by spin transfer from the positions of molecule farther from the oxygen atoms to places closer to them. As we discussed above, the electron-withdrawing NO_2 substituent reduces the overall spin density of SQ, but as can be seen from Table III, the individual proton couplings can even increase. In particular, for 2,7-$(NO_2)_2$ substitution, where an increased spin density can be ascribed to the oxygen atoms, the larger proton couplings, i.e. the larger spin densities, can be assigned to the carbons closer to the oxygen atoms:

$$a_{1,8} > a_{3,6} \tag{4}$$

In the case of 2,7,-di-*tert*-butyl substitution, the assignment is just the opposite.

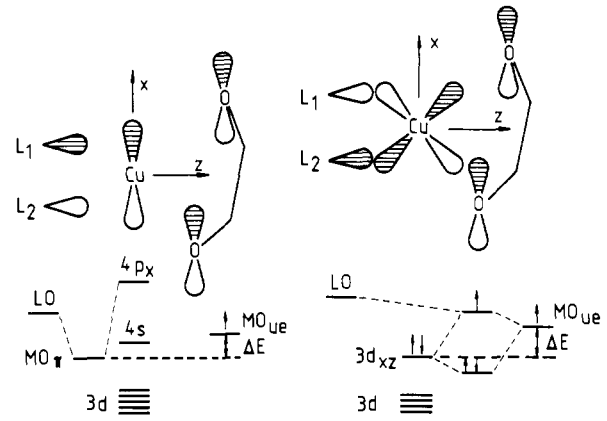

Figure 5. Molecular orbital bonding schemes proposed by Razuvaev (left) and in this paper (right).

It is noteworthy that the sum of couplings $a_1 + a_3 + a_6 + a_8$ is larger for the complexes than for the anion radical though the spin delocalization is evidently larger in the former case. This fact can be explained by the charge neutralization reducing the net charge of SQ, and for neutral radicals the hyperfine constant is significantly larger than for anion radicals if the spin density is the same.[14]

Discussion

The preceding analysis shows the spectra data vary oppositely than expected on the basis of electron affinity of SQ. This statement can be extended from the change of spin density on the metal ion and the neutral ligand to the rearrangement of spin density on the skeleton of SQ, too. Razuvaev[1] proposed a molecular orbital (MO) scheme in order to explain this anomalous phenomenon. In this model a strong π-bonding was assumed, which consists of the unpaired electron MO of semiquinone (MO_{ue}), the $4p_x$ orbital of the copper ion, and the antisymmetric group orbital of the two neutral ligands (LO) in the $[CuL_2(SQ)]$ complex (Figure 5 (left)). In this model the π-bonding between the LO and the Cu $4p_x$ orbital is assumed strong enough for inverting the energy order of LO_π and MO_{ue}, where LO_π is the respective π-bonding orbital between the neutral ligands and copper ion. If this inversion takes place, then the lowering of MO_{ue} energy due to the increased electron affinity of SQ will reduce the separation between MO_{ue} and LO_π, which affords stronger bonding between SQ and Cu and larger spin transfer from SQ to the metal ion and neutral ligand. In the case of the complex $[CuL(SQ)]$, the trigonal symmetry does not allow formation of the above π-bond, which prevents the spin transfer to the metal ion and neutral ligands.

Though the major trends of spin transfer can be explained by the above model, there remain a few shortcomings. In particular, if the energy orders of LO_π and MO_{ue} were different for complexes $[CuL(SQ)]$ and $[CuL_2(SQ)]$, then for the solvent-coordinated complexes $[CuL(S)(SQ)]$, where the assumed π-bonding between the LO and the Cu $4p_x$ orbital should be of intermediate strength, the energies of the respective orbitals can be nearly equal, which might yield to stronger covalent bond and larger spin transfer between SQ and the metal ion in this case than in the bis(triphenylphosphine) complex. This expectation, however, contradicts the conclusions that can be drawn from Figure 3. Razuvaev's model also fails to explain the complex rearrangement of spin distribution on the semiquinone skeleton: only a uniform depletion of spin densities is expected if the electron affinity of SQ is increased by using electronegative substituents. Moreover, it is quite unlikely the π-bond assumed by Razuvaev can be very strong, since in the case of tetrahedral coordination the $4s4p^3$ hybrid orbitals of the copper ion can form σ-bonds, as well.

We think the anomalous direction of spin density variation is related to the role of 3d orbitals in the formation of weak π-bonds.

(13) Prabhananda, B. S. *J. Chem. Phys.* **1983**, 79, 5752.

(14) Bolton, J. R. *J. Chem. Phys.* **1965**, *43*, 309.

If the geometry is tetrahedral, among 3d orbitals of the highest energy, the $3d_{xz}$ orbital can form π-bonding with the π-system of SQ (Figure 5 (right)). Since all 3d orbitals are doubly occupied, while MO_{ue} is singly occupied, there are two electrons on the bonding orbital and one in the antibonding orbital, if a covalent bond is formed. Consequently, the net electronic charge changes in the direction opposite to that of the spin density: the transfer of $3d_{xz}$ electron pair from the metal ion into SQ is accompanied by the transfer of an unpaired electron from SQ to the metal ion. In particular, if a substituent enlarges the electron affinity of SQ, then its negative charge density increases and its spin density decreases, while the variation of these densities takes place in the opposite direction on the metal ion and neutral ligands. Concerning the spin distribution on the SQ skeleton, the spin density is large on those atoms where the charge density is enhanced owing to the $3d_{xz}$ electron pair transport. The larger spin transfer in the complexes $[Cu(SQ)L_2]$ than in the complexes $[Cu(SQ)L]$ can also be explained in our model: the energy of the $3d_{xz}$ orbital is much larger in the tetrahedral ligand field than in the trigonal field, which makes the separation of $3d_{xz}$ and MO_{ue} orbitals smaller and the respective π-bond stronger, and consequently, more charge is transported to SQ and more spin density to the metal ion and neutral ligands.

Registry No. **1**, 65123-87-7; **2**, 109959-92-4; **3**, 109959-93-5; **4**, 109959-94-6; **5**, 109959-95-7; **6**, 109959-96-8; **7**, 109959-97-9.

Contribution from the Department of Chemistry and Ipatieff Catalytic Laboratory, Northwestern University, Evanston, Illinois 60201

Synthesis of Lithium Dialuminate by Salt Imbibition

K. R. Poeppelmeier* and S.-J. Hwu

Received December 30, 1986

The synthesis of lithium dialuminate $LiAl_2(OH)_7 \cdot 2H_2O$ by reaction at room temperature of solid lithium hydroxide, polycrystalline aluminum trihydroxide (bayerite), and water vapor is described. The aluminate prepared by this method has been characterized by chemical analysis, thermogravimetric analysis, infrared spectroscopy, and X-ray powder diffraction and appears to be identical with that prepared by precipitation from supersaturated aluminate solutions or by reaction of lithium salts with freshly precipitated aluminum hydroxide in aqueous solution. All current evidence suggests that the structure of lithium dialuminate is like that of hydrotalcite, $[Mg_6Al_2(OH)_{16}]^{2+}CO_3^{2-} \cdot 4H_2O$, with neutral dioctahedral sheets of bayerite converted to positively charged trioctahedral layers by incorporation of lithium ion. Hydroxide ion and two water molecules reside between the layers and presumably approximate a plane of oxygen atoms stabilized by hydrogen bonding, as evidenced by a 2.81 (1) Å increase in the bayerite lattice perpendicular to the dioctahedral layer. A more descriptive chemical formula for lithium dialuminate would be $[LiAl_2(OH)_6]^+OH^- \cdot 2H_2O$. The imbibition of other lithium salts (LiX; X = Cl^-, Br^-, I^-, NO_3^-) was also studied. Thermal decomposition results in compounds, related to the transitional aluminas, with high specific surface area and porosity.

Introduction

Hydrated lithium dialuminate, $LiAl_2(OH)_7 \cdot 2H_2O$, precipitates[1] from a solution prepared by dissolving aluminum metal in hot lithium hydroxide and was originally formulated to be an "acid" aluminate $LiH(AlO_2)_2 \cdot 5H_2O$. Subsequent investigators used conductometric measurements to study the soluble species $Al(OH)_4^-$ and $Al_2(OH)_7^-$ and suggested[2] that the formula should reflect two molecules of water loosely bound as waters of crystallization, with the remaining water bound directly to the aluminum cations. Later it was shown[3] that pH and lithium ion concentration could be varied over a considerable range without an effect on the composition of the insoluble compound. Recently[4] it has been shown that the dialuminate compound $LiAl_2(OH)_7 \cdot 2H_2O$ is not the only compound that can be isolated from aqueous solution. The reaction of hydrated lithium dialuminate at 90 °C with a concentrated sodium hydroxide solution is reported to result in crystalline lithium monoaluminate with the approximate chemical composition $Li_2O \cdot Al_2O_3 \cdot nH_2O$ with $n \sim 0.5$.

Of considerable technological importance are factors that determine the nature of the particular aluminum hydroxide phase to precipitate from solution such as the type and amount of alkali-metal ion present, temperature, and pH. Bayerite and pseudoboehmite are precipitated in the presence of Na^+, K^+, and Cs^+ ions. In the presence of Li^+ ions[5,6] pseudoboehmite does not readily form, and a selective and accelerated precipitation of bayerite is observed at low Li^+ ion concentrations, whereas at low supersaturation and high Li^+ concentrations bayerite formation is preceded by $LiAl_2(OH)_7 \cdot 2H_2O$ precipitation.

Powder X-ray diffraction patterns have been reported for both the mono- and dialuminates.[4,7] Recently a structural model that does not require all the hydroxide ions to be bound to the aluminum cations has been proposed[8] for the hydrated lithium dialuminate. In a study of the hydrolysis of Al^{3+} in carbonate salt solutions the compound $[LiAl_2(OH)_6]_2^+CO_3^{2-} \cdot nH_2O$ was isolated. On the basis of electron diffraction, X-ray powder diffraction, and infrared studies, it was suggested that these dialuminates are derivatives of $Al(OH)_3$ where aluminum cations occupy two-thirds of the octahedral sites between sheets of close-packed hydroxide ions and lithium cations fill the remaining octahedral sites (one-third). That is, the compound $LiAl_2(OH)_7 \cdot 2H_2O$ is a layered double hydroxide. The more descriptive formula $[LiAl_2(OH)_6]^+OH^- \cdot 2H_2O$ emphasizes the fact that the one additional hydroxide ion is an interlayer anion. Ideally, two molecules of water also occupy the interlayer region in this compound.

Because the structure of these hydrotalcite-like compounds are conceptually derived from that of crystalline $Al(OH)_3$ (e.g., bayerite), we considered the direct reaction of $LiOH \cdot H_2O(s)$ with $Al(OH)_3(s)$. Reactions of alumina gels (gibbsite, bayerite, or norstandite) with lithium salts in aqueous media have been reported.[9,10] The general formula of the products was proposed to be $(LiX_x)_y \cdot 2Al(OH)_3 \cdot nH_2O$, where n is the number of waters of hydration, y is the number of lithium atoms present for each 2 mol of aluminum, and x is the reciprocal of the valence of the anion. The value for y was reported in the range $0.5 \leq y \leq 1.2$.

(1) Allen, E. T.; Rogers, H. F. *Am. Chem. J.* **1900**, *24*, 304.
(2) Prociv, D. *Collect. Czech. Chem. Commun.* **1929**, *1*, 95.
(3) Horan, H.; Damiano, J. B. *J. Am. Ceram. Soc.* **1935**, *57*, 2434.
(4) Lileev, I. S.; Sachenko-Sakun, L. K.; Guseva, I. V. *Russ. J. Inorg. Chem.* **1968**, *13*(2), 213.
(5) Frenkel, M.; Glasner, A.; Sarig, S. *J. Phys. Chem.* **1980**, *84*, 507.
(6) Van Straten, H. A.; Schoonen, M. A. A.; De Bruyn, P. L. *J. Colloid, Interface Sci.* **1985**, *103*, 493.
(7) Gorin, P.; Marchon, J.-C.; Tranchant, J.; Kovacevic, S.; Marsault, J.-P. *Bull. Soc. Chim. Fr.* **1970**, 3790.
(8) Serna, C. J.; Rendon, J. L.; Iglesias, J. E. *Clays Clay Miner.* **1982**, *30*, 180.
(9) Bauman, W. C.; Lee, J. M.; Burba, J. L. U.S. Patent 4 348 296, 1982.
(10) Bauman, W. C.; Lee, J. M. U.S. Patent 4 348 297, 1982.

0020-1669/87/1326-3297$01.50/0